Engineered receptor binding domain immunogens elicit pan-sarbecovirus neutralizing antibodies outside the receptor binding motif

Blake M. Hauser[1#], Maya Sangesland[1#], Evan C. Lam[1], Kerri J. St. Denis[1], Jared Feldman[1], Ashraf S. Yousif[1], Timothy M. Caradonna[1], Ty Kannegieter[1], Alejandro B. Balazs[1], Daniel Lingwood[1*] and Aaron G. Schmidt[1,2*]

Affiliations:

[1]Ragon Institute of MGH, MIT and Harvard, Cambridge, MA, 02139, USA

[2]Department of Microbiology, Harvard Medical School, Boston, MA 02115, USA

*Correspondence to: Aaron G. Schmidt (aschmidt@crystal.harvard.edu), Daniel Lingwood (dlingwood@mgh.harvard.edu)

# These authors contributed equally.

Abstract: Effective countermeasures are needed against emerging coronaviruses of pandemic potential, similar to severe acute respiratory syndrome coronavirus 2 (SARS-CoV-2). Designing immunogens that elicit broadly neutralizing antibodies to conserved viral epitopes on the major surface glycoprotein, spike, such as the receptor binding domain (RBD) is one potential approach. Here, we report the generation of homotrimeric RBD immunogens from different sarbecoviruses using a stabilized, immune-silent trimerization tag. In mice, we find that a cocktail of these homotrimeric sarbecovirus RBDs elicits antibodies to conserved viral epitopes outside of the ACE2 receptor binding motif (RBM). Importantly, these responses neutralize all sarbecovirus components even in context of prior SARS-CoV-2 imprinting. We further show that a substantial fraction of the neutralizing antibodies elicited after vaccination in humans also engages non-RBM epitopes on the RBD. Collectively, our results suggest a strategy for eliciting broadly neutralizing responses leading to a pan-sarbecovirus vaccine.

Short title: Eliciting pan-coronavirus neutralizing antibodies after SARS-CoV-2 imprinting

Author summary: Immunity to SARS-CoV-2 in the human population will be widespread due to natural infection and vaccination. However, another novel coronavirus will likely emerge in the future and may cause a subsequent pandemic. Humoral responses induced by SARS-CoV-2 infection and vaccination provide limited protection against even closely related coronaviruses. We show immunization with a cocktail of trimeric coronavirus receptor binding domains induces a neutralizing antibody response that is broadened to related coronaviruses with pandemic potential. Importantly, this broadening occurs in context of an initial imprinted SARS-CoV-2 spike immunization showing that preexisting immunity can be expanded to recognize other related

37 coronaviruses. Our immunogens focused the serum antibody response to conserved epitopes on
38 the receptor binding domain outside of the ACE2 receptor binding motif; this contrasts with
39 current SARS-CoV-2 therapeutic antibodies, which predominantly target the receptor binding
40 motif.

41 **Main Text:**

42 **Introduction**

43 The emergence of the novel severe acute respiratory syndrome coronavirus 2 (SARS-CoV-2) and
44 the subsequent global pandemic has highlighted the disruptive threat posed by viruses for which
45 humans have no prior immunity. Rapid development of potential vaccines has led to an
46 unprecedented 40 candidates already in Phase 3 clinical trials or approved since January 2020;
47 while differing in modality (e.g., mRNA, adenovirus), the primary immunogen for many of these
48 candidates is the SARS-CoV-2 spike ectodomain (1). With the continued global spread of SARS-
49 CoV-2, in conjunction with potential vaccinations, it is likely that a large proportion of the global
50 population will eventually develop an immune response to SARS-CoV-2. However, even after
51 potentially achieving herd immunity sufficient to slow the spread of SARS-CoV-2, there remains
52 a constant threat of emerging coronaviruses with pandemic potential. Indeed, surveillance efforts
53 have identified numerous unique coronaviruses within various animal reservoirs, raising the
54 possibility of zoonotic transmission (2, 3). Such events are likely to increase in frequency as a
55 result of human impact on the environment (4). While the current SARS-CoV-2 pandemic has an
56 estimated infection fatality rate of between ~1-2%, with numerous cases likely undetected,
57 previous SARS-CoV and MERS-CoV outbreaks were more lethal with ~10% and ~35% case
58 fatality rates, respectively, raising the possibility that future novel coronaviruses will potentially
59 have high mortality (5-7). Additionally, elicited immunity to SARS-CoV-2 infection may not
60 protect against even closely related novel coronaviruses from the same sarbecovirus subgenus (8,
61 9). It is therefore critical to not only address the current pandemic, but also develop vaccine
62 platforms that can be readily adapted to potential emerging coronaviruses.

63

While we cannot readily predict which coronaviruses will next emerge into the human population, a proactive approach to generate broadly protective immunity is to design immunogens that elicit humoral responses targeting conserved sites on the coronavirus spike glycoprotein. Such sites may include the receptor binding domain which engages host-cell receptors necessary to facilitate viral cell entry; these spike-mediated interactions are conserved across coronaviruses (10). Indeed, a subset of spike-directed antibodies from convalescent patients can potently neutralize SARS-CoV-2; comparable neutralizing antibodies against SARS-CoV and MERS-CoV have also been identified (6, 11-16). Some spike-directed antibodies that neutralize SARS-CoV-2 also bind the SARS-CoV spike protein, highlighting the presence of cross-reactive neutralizing epitopes (11, 17, 18). Multimerized versions of the receptor binding domains (RBDs) of several coronaviruses have previously been shown to be potent immunogens (19). Here, we describe a customizable vaccine that elicits pan-sarbecovirus neutralization against both SARS-CoV-2 and the potentially emergent WIV1-CoV (20). This approach focuses antibody responses to conserved, protective RBD epitopes shared across sarbecoviruses. Its flexible nature allows facile interchanging of potential vaccine strains updated to confer neutralization against new emerging coronaviruses. Responses focused to these conserved epitopes maintain potent SARS-CoV-2 neutralization activity despite minimal ACE2 receptor binding motif coverage. Importantly, this approach was applied in context of "pre-existing" SARS-CoV-2 humoral immunity with the goal of broadening neutralization while simultaneously boosting the neutralizing antibody response to SARS-CoV-2, similar to the "back boost" effect of seasonal influenza immunizations (21). Thus, it has the potential to provide protection against currently circulating SARS-CoV-2, while proactively generating neutralizing antibody responses against emerging coronaviruses.

87 **Results**

88 *Designing a Trimerized Receptor Binding Domain Construct Using a Non-Immunogenic Tag*

89 We designed a cystine-stabilized and hyperglycosylated variant of a GCN4 trimerization tag to
90 generate a homotrimeric immunogen "cassette" to rapidly exchange RBDs from various
91 coronaviruses (**Fig. 1A**). While the two cysteines are within one subunit, they are engineered to
92 form an intermolecular disulfide with an adjacent subunit when the trimer is formed. Using a
93 hyperglycosylated GCN4 allows the RBDs to remain trimerized while the tag is "immune silent"
94 (22). As a proof-of-concept for our immunization approach, we selected the SARS-CoV, SARS-
95 CoV-2, and WIV1-CoV RBDs as our starting immunogens. We overexpressed RBD homotrimers
96 in mammalian cells (Expi293F cells) to maximize glycan complexity and purified to homogeneity
97 via immobilized metal affinity chromatography followed by size exclusion chromatography; the
98 trimeric species was confirmed using SDS-PAGE analysis under non-reducing conditions (**Fig.
99 1B-C**). Their antigenicity was assayed using conformational-specific antibodies CR3022 and/or
100 B38 using biolayer interferometry; the RBD homotrimers had comparable affinities in comparison
101 to RBD monomers (**Fig. S1**). The 8xHis purification tags were removed by HRV 3C protease
102 enzymatic cleavage prior to immunization.

103

104 *Immunization Regimens Generate Cross-Reactive Antibody Responses*

105 To understand how preexisting immunity to SARS-CoV-2, whether acquired through natural
106 infection or vaccination, could affect immune responses to our immunogens, we primed our
107 cohorts with recombinant spike or RBD protein (23, 24). Our two control arms followed this prime
108 with subsequent homologous boosts of recombinant SARS-CoV-2 spike ("Spike" cohort) or RBD
109 ("RBD" cohort); the latter is necessary for comparing the effect on immunogencity of monomeric

110 versus trimeric RBDs. Our experimental arms both received the spike prime and included a SARS-
111 CoV-2 RBD homotrimer boost ("Homotrimer" cohort) and an equimolar boosting cocktail of
112 SARS-CoV-2, SARS-CoV, and WIV1-CoV RBD homotrimers ("Cocktail" cohort) (**Fig. 2A**). All
113 cohorts received the same total amount of protein in each immunization, 20 μg, adjuvanted with
114 Sigma Adjuvant (25). Immunizations were performed at days 0, 21, and 42. We evaluated the
115 serum response against coronavirus-derived antigens using ELISAs, including SARS-CoV-2
116 spike, RBDs from SARS-CoV-2, SARS-CoV, WIV1, as well as a SARS-CoV-2 ΔRBM RBD with
117 two engineered glycans that abrogate ACE2 engagement (**Fig. 2B, S2A, S3A-C**). All four
118 immunization regimens resulted in similar patterns of serum reactivity. Each cohort demonstrated
119 a significant decrease in reactivity against SARS-CoV RBD as compared to the SARS-CoV-2
120 RBD or spike, though the magnitude of this difference was relatively small. The cohort which
121 received the RBD homotrimer cocktail boost had the highest overall endpoint titers, while the
122 cohort that received the monomeric SARS-CoV-2 RBD had the lowest overall endpoint titers; the
123 latter observation is consistent with other previous reports and likely due to the inefficiency of
124 monomeric RBDs effectively stimulating B cell receptors. We confirmed the non-immunogenic
125 nature of the hyperglycosylated GCN4 tag by assaying sera from the wildtype homotrimer cocktail
126 boost against another viral glycoprotein, hemagglutinin, with the same tag (**Fig. S2B**).
127
128 *Immunization with a Cocktail of Homotrimeric Receptor Binding Domains Focuses the Immune*
129 *Response to Cross-Reactive Epitopes*
130 We next evaluated whether the serum response was directed towards cross-reactive, and
131 potentially broadly neutralizing RBD epitopes. Conservation across SARS-CoV-2, SARS-CoV,
132 and WIV1-CoV RBDs primarily occurs outside of the ACE2 receptor binding motif (RBM).

133 Indeed, the previously characterized CR3022 and S309 antibodies have footprints that together
134 cover much of this conserved region, with epitope buried surface area (BSA) of 917 $Å^2$ and 795
135 $Å^2$ respectively in comparison to BSA of 869 $Å^2$ for ACE2 (17, 18, 26). We performed serum
136 competition by incubating RBD-coated ELISA plates with IgGs B38, P2B-2F6, CR3022, and
137 S309, representing each of the four previously defined "classes" of SARS-CoV-2 RBD epitopes
138 (27) (**Fig. S2C**). We then assessed binding of mouse serum IgG. In all cohorts, competition with
139 both CR3022 and S309 significantly reduced serum titers against the SARS-CoV and WIV1-CoV
140 RBDs (**Fig. 2C, S2C**). However, only the cohort receiving the RBD homotrimer cocktail showed
141 a significant reduction in serum titers against the SARS-CoV-2 RBD in competition with both
142 CR3022 and S309 ($p = 0.0340$) (**Fig. 2C**). This result suggests a higher degree of focusing to this
143 region elicited specifically by the homotrimer cocktail immunogens.
144
145 *Expanded IgG B Cell Populations Target Cross-Reactive Receptor Binding Domain Epitopes*
146 To compare the observed sera responses, we measured the amount of antigen-specific IgG B cells
147 expanded by the Spike, Homotrimer, and Cocktail immunization regimens. Low antigen-specific
148 ELISA titers for the RBD cohort indicated that we were unlikely to be able to robustly quantitate
149 antigen-specific B cells, therefore mice from that cohort were excluded from subsequent analyses.
150 We engineered a SARS-CoV-2 RBD variant that has two additional glycans on the RBM which
151 effectively block ACE2 engagement (**Fig. S3A-C**). This variant allowed us to bin SARS-CoV-2
152 spike-directed B cells into 3 populations: those that bound RBM epitopes; those that bound the
153 non-RBM epitopes on the RBD; and those that bound the "remainder" of the spike protein (**Fig.
154 S3D-E**). As a subset of SARS-CoV-2 spike-directed B cells, the proportion of B cells specific for
155 the SARS-CoV-2 RBM and non-RBM portion of the RBD were considerably higher in the cohorts

156 receiving the SARS-CoV-2 RBD homotrimer and RBD homotrimer cocktail boosts (p = 0.0070)
157 (**Fig. 3A**). We also binned B cells that bound to both the SARS-CoV-2 spike and either the SARS-
158 CoV RBD or WIV1-CoV RBD (**Fig. 3B**). We found that cross-reactive IgG B cells predominantly
159 targeted epitopes outside the RBM (the spike remainder a result of the prime), mirroring what we
160 observed in sera responses.
161
162 *Elicited Immune Response is Cross-Neutralizing and Targets Non-Receptor Binding Motif*
163 *Epitopes*
164 We next determined the neutralization potency from each of our cohorts using SARS-CoV-2,
165 SARS-CoV, and WIV1-CoV pseudoviruses (8, 9). We obtained NT50 values when possible; we
166 note that most serum samples for which NT50 values could not be determined still had some weak
167 neutralizing activity (20 out of 24 samples) (**Fig. S4E**). We observed a significant increase in
168 WIV1-CoV neutralization in the cohort that received the homotrimer cocktail boost compared to
169 all other cohorts (p = 0.0012) (**Fig. 4A**). Importantly, this did not result in any significant loss in
170 serum neutralization potency against SARS-CoV-2 (p = 0.6594) (**Fig. 4B**). We also observed
171 higher levels of SARS-CoV neutralization in the cohort that received the homotrimer cocktail
172 boost as compared to the cohort boosted with the SARS-CoV-2 RBD homotrimer and the SARS-
173 CoV-2 monomeric RBD, though this trend was not significant (p = 0.2370) (**Fig. 4C**). The samples
174 from the cohort that received the homotrimer cocktail boost where an NT50 value could not be
175 obtained, nevertheless still show some evidence of weak neutralization.
176
177 To assess cross-neutralization of related coronaviruses that were not included in the RBD
178 homotrimer cocktail cohort, we performed neutralization assays using RaTG13-CoV and

179 SHC014-CoV pseudoviruses, both of which are members of the sarbecovirus subgenus that have
180 been detected in bats but not in humans (**Fig. 4D**) (28, 29). These viruses, along with WIV1, are
181 ACE2-using sarbecoviruses in animal reservoirs that could enter the human population, similar to
182 SARS-CoV and SARS-CoV-2. RaTG13-CoV is closely related to SARS-CoV-2 with 89.6%
183 amino acid identity within the RBD, while SHC014 is more distant with 76.3% identity. For
184 RatG13-CoV, we observed similar neutralization patterns whereby the RBD cohort had
185 significantly lower neutralization than the Spike and Cocktail cohorts. (**Fig. 4D-E**). For SHC014-
186 CoV, however, the cohort that received the RBD homotrimer cocktail boosts showed significantly
187 greater neutralization compared to all other cohorts ($p = 0.0145$) (**Fig. 4D, F**). Furthermore, the
188 corresponding ELISA titers also show no loss in binding to the SHC014-CoV and RaTG13-CoV
189 RBDs relative to SARS-CoV-2 RBD (**Fig. S2D-E**). Thus, compared to other cohorts,
190 immunization with the RBD homotrimer cocktail resulted in a neutralizing antibody response with
191 both retrospective (e.g., SARS-CoV) and prospective breadth (e.g., WIV1-CoV, SHC014-CoV,
192 and RaTG13-CoV) even in context of preexisting immunity to SARS-CoV-2.
193
194 We wanted to determine what fraction of SARS-CoV-2 neutralization could be attributed to the
195 non-RBM RBD-directed response. To that end, we performed adsorption of pooled sera from each
196 cohort using MERS-CoV RBD (negative control), SARS-CoV-2 RBD, and a SARS-CoV-2 RBD
197 with four additional glycans engineered onto the RBM (SARS-CoV-2 ΔRBM RBD) (**Fig. S3B,**
198 **S4A-D**). This construct was designed to block all RBM-directed antibodies as opposed to the one
199 used in flow cytometry, which only block antibodies that directly compete with ACE2. Samples
200 adsorbed with all three RBD constructs showed decreased neutralization compared to serum due
201 to the dilution involved in the adsorption protocol. Compared to the samples adsorbed using MERS

202 RBD, the samples adsorbed with either the SARS-CoV-2 RBD or the SARS-CoV-2 ΔRBM RBD
203 demonstrated a significant loss of SARS-CoV-2 neutralization ($p = 0.0343$) (**Fig. 4G, S4E**). This
204 indicates that non-RBM RBD-directed antibodies alone are able to confer significant SARS-CoV-
205 2 neutralization. We performed similar adsorption experiments on 24 post-vaccination human
206 serum samples from a previously characterized vaccine cohort (9). These patients had received
207 either 1 or 2 doses of the Pfizer (BNT162b2) or Moderna (mRNA-1273) vaccines. Similar to our
208 murine observations, human samples adsorbed using either the SARS-CoV-2 RBD or the SARS-
209 CoV-2 ΔRBM RBD lost significant neutralization compared to samples adsorbed using MERS
210 RBD ($p = 0.0253$) (**Fig. 4H**). Still, samples adsorbed with SARS-CoV-2 ΔRBM RBD did show
211 higher neutralization activity relative to samples adsorbed with SARS-CoV-2 RBD across both
212 the human and mouse samples. This indicates that RBM- and non-RBM antibodies targeting the
213 RBD play important roles in conferring SARS-CoV-2 neutralization.
214
215 **Discussion**
216
217 Here, we demonstrate that a cocktail of homotrimeric sarbecovirus RBDs can effectively generate
218 a neutralizing response to all components and additional related sarbecoviruses without a bias
219 resulting from an initial SARS-CoV-2 imprinting. We find that this cross-neutralizing antibody
220 response is predominantly directed to RBD epitopes outside of the RBM. This contrasts SARS-
221 CoV-2 infection which does not appear to reliably generate cross-neutralizing antibodies (8, 9).
222 Previous analysis into the epitopes targeted by this cross-neutralizing response has not been
223 conducted (30). Furthermore, previously reported vaccine candidates that aim to generate such a
224 cross-neutralizing response have not been shown to successfully focus immunity towards cross-

225 neutralizing epitopes following an initial SARS-CoV-2 spike immunization, but instead were
226 tested only in a naïve homologous prime/boost format (30). However, our results suggest that
227 following an initial SARS-CoV-2 exposure (e.g., vaccination, infection), subsequent boosting with
228 a surveillance-informed selection of sarbecovirus RBD homotrimers could result in pan-
229 sarbecovirus immunity that protects against future pandemics despite targeting non-RBM
230 epitopes. Whereas currently available vaccine candidates, particularly mRNA-based vaccines,
231 appear to largely provide effective protection against currently circulating SARS-CoV-2 variants
232 of concern, it remains unclear whether currently approved vaccines will provide protection against
233 emerging sarbecoviruses (31-35). Immunization with SARS-CoV-2 spike-based vaccines, as well
234 as SARS-CoV-2 infection, results in a significant loss in neutralization against existing pre-
235 emergent sarbecoviruses in both humans and animal models (8, 9, 36). SARS-CoV-2 spike-based
236 vaccines also have reduced *in vivo* protection against SARS-CoV and WIV1 compared to SARS-
237 CoV-2 (36).
238
239 Monomeric as well as numerous SARS-CoV-2 multimerized RBD-based vaccine constructs have
240 been published recently and are in various stages of preclinical and clinical testing (19, 30, 37-44).
241 However, these multimerization platforms present additional epitopes that can give rise to a
242 scaffold-specific antibody response, which has the potential to alter hierarchies of
243 immunodominance. Our non-immunogenic hyperglycosylated, cystine-stabilized GCN4 tag
244 improves upon a previous hyperglycosylated version of the tag that showed markedly reduced
245 immunogenicity (22). This may be due to the implementation of cystine-stabilization limiting the
246 accessibility of epitopes within the coiled-coil interface of the GCN4 tag that may not be fully
247 shielded by engineered glycans.

248

249 This immunogen cocktail provides a framework upon which further studies to optimize a pan-
250 coronavirus vaccine can build to generate optimal broadly neutralizing antibody responses. This
251 could include antibodies targeting the N-terminal domain as well as the RBD, possibly elicited by
252 vaccine regimens including full-length spike proteins. SARS-CoV-2 pseudovirus neutralization
253 assays may underestimate the contributions of antibodies that target epitopes outside the RBD,
254 though it remains unclear the extent to which this occurs when measuring a polyclonal serum
255 response and against other coronaviruses (45-47). Still, most potently neutralizing monoclonal
256 antibodies and immunization-elicited neutralizing antibodies in humans receiving the approved
257 mRNA vaccines appear to target the RBD, emphasizing the importance of shaping the RBD-
258 directed immune response with any potential future boosting immunizations given the likely
259 impending ubiquity of vaccine-elicited immunity (48-51).

260

261 While the durability of vaccine or infection-elicited antibody responses to SARS-CoV-2 remains
262 to be seen, data from seasonal coronaviruses, as well as SARS-CoV and MERS-CoV, suggests
263 that immunity appears to wane after several years and can vary in potency between individuals
264 (52-58). Thus, if herd immunity is not achieved or if antigenic drift of SARS-CoV-2 necessitates
265 reformulation of current vaccines, it may present an opportunity to incorporate immunogens based
266 on emerging coronaviruses identified through surveillance (20); importantly, based on the data
267 presented here, such incorporation would not be at the detriment of neutralizing activity against
268 SARS-CoV-2. Assessing *in vivo* protection efficacy of this vaccine regimen against SARS-CoV-
269 2, in context of preexisting immunity to SARS-CoV-2, is hindered by the observation that a single
270 SARS-CoV-2 spike immunization alone provides notable *in vivo* protection (59).

271

272 In addition to informing future immunization regimens, these findings demonstrate that potent
273 cross-neutralizing antibodies can target epitopes outside of the RBM on the SARS-CoV-2 RBD.
274 Our results further demonstrate that non-RBM neutralization via the RBD forms a significant
275 fraction of SARS-CoV-2 immunity elicited in in humans. Many potently neutralizing monoclonal
276 antibodies currently in therapeutic development target RBM epitopes in regions of the RBD with
277 minimal conservation across members of the sarbecovirus subgenus (48, 51). Consequently, these
278 antibodies are unlikely to provide protection against future emerging coronaviruses. Identifying
279 neutralizing antibodies targeting conserved epitopes outside the RBM and the appropriate
280 immunizations strategies and modalities to elicit them may provide the broad protection necessary
281 for pan-coronavirus immunity (11, 18, 49). Furthermore, targeting these non-RBM, but still
282 conserved epitopes, may also reduce the likelihood of antibody escape, which have already been
283 documented for existing SARS-CoV-2 monoclonal antibodies (45, 60). Immunogens that facilitate
284 immune focusing to conserved RBD epitopes, while still presenting the SARS-CoV-2 RBM, can
285 generate a cross-neutralizing antibody response in addition to eliciting SARS-CoV-2-directed
286 antibodies belonging to the potently neutralizing classes of RBM-directed antibodies.

287

288 While the currently approved vaccines use an mRNA platform to present SARS-CoV-2 spike,
289 additional immunization strategies use protein-based multivalent constructs (19, 30, 37).
290 Collectively these efforts are designed to elicit both SARS-CoV-2 and, in some cases, pan-
291 coronavirus immunity. The approach described here demonstrates a potential alternate but
292 complementary path to generate neutralizing antibodies against multiple sarbecoviruses even in
293 the context of prior immunity to SARS-CoV-2. Furthermore, this cocktail-based approach using

trimeric immunogens parallels the current influenza vaccine composition, which aims to elicit broad immunity to each constituent strain. This proof-of-principle study indicates that a similar surveillance-based approach could be applied to future coronavirus vaccines, that protect against future emerging coronaviruses while also maintaining protection against SARS-CoV-2.

301 **Materials and Methods**

302 Receptor Binding Domain and Homotrimer Expression and Purification

303 Receptor binding domains (RBDs) were designed based on the following sequences: SARS-CoV-
304 2 RBD (Genbank MN975262.1), SARS-CoV RBD (Genbank ABD72970.1), WIV1-CoV RBD
305 (Genbank AGZ48828.1), and MERS-CoV RBD (Genbank AHI48572.1). Constructs were codon
306 optimized by Integrated DNA Technologies, cloned into pVRC, and sequence confirmed by
307 Genewiz. The spike plasmid was obtained from Dr. Jason McLellan at the University of Texas,
308 Austin. It contained a Foldon trimerization domain as well as C-terminal HRV 3C-cleavable 6xHis
309 and 2xStrep II tags. Proteins were expressed in Expi293F cells (ThermoFisher) using
310 Expifectamine transfection reagents according to the manufacturer's protocols. All proteins
311 included a C-terminal HRV 3C-cleavable 8xHis tag to facilitate purification. Monomeric RBD
312 proteins also contained SBP tags, while homotrimeric constructs contained a previously published
313 hyperglycosylated GCN4 tag with two additional C-terminal cystines (22). A linker with the
314 sequence GAGSSGSG separated each RBD from the hyperglycosylated GCN4 tag. Versions of
315 the MERS-CoV RBD, SARS-CoV-2 ΔRBM RBD with four additional putative glycosylation sites
316 (Figure S5), and SARS-CoV-2 RBD with C-terminal 8xHis and SNAP tags (61) were also
317 generated.

318

319 Transfections were harvested after 5 days and clarified via centrifugation. Cell supernatants were
320 passaged over Cobalt-TALON resin (Takara) for immobilized metal affinity chromatography via
321 the 8xHis tag. After elution, proteins were passed over a Superdex 200 Increase 10/300 GL (GE
322 Healthcare) size exclusion column in PBS (Corning). Prior to immunization, 8xHis tags were
323 cleaved using HRV 3C protease (ThermoScientific). Cleaved protein was repurified using Cobalt-

324 TALON resin in order to remove the protease, cleaved tag, and any uncleaved protein.
325 Approximate purified homotrimer yields per liter of Expi293F transfected were as follows: SARS-
326 CoV-2 – 3 mg; SARS-CoV – 20 mg; WIV1-CoV – 25 mg.
327
328 Fab and IgG Expression and Purification
329 Genes for the variable domains of the heavy and light chains were codon optimized by Integrated
330 DNA Technologies and cloned into pVRC constructs containing the respective constant domains
331 as previously described (62, 63). Heavy-chain Fab constructs contained a HRV 3C-cleavable
332 8xHis tag, while heavy-chain IgG constructs contained HRV 3C-cleavable 8xHis and SBP tags.
333 Transfections and purifications were performed according to the same protocols used for the RBDs
334 and homotrimers.
335
336 Biolayer Interferometry
337 Biolayer interferometry (BLI) experiments were performed using a BLItz instrument (ForteBio).
338 Fabs were immobilized on a FAB2G biosensor (ForteBio), and CoV proteins were the analytes.
339 All proteins were diluted in PBS at room temperature. Titrations were performed to determine
340 binding affinities. Single-hit concentrations at 10 μM were performed to get an approximate K_D,
341 and then subsequent titrations at appropriate concentrations (at least three). A final K_D estimate
342 was determined using a global fit model with a 1:1 binding isotherm using vendor-supplied
343 software.
344
345 Immunizations

346 C57BL/6 mice (Jackson Laboratory) received 20 μg of protein adjuvanted with 50% w/v Sigma
347 Adjuvant System in 100 μL of inoculum (25). All immunizations were administered through the
348 intraperitoneal route. Mice were primed (day 0) and received boosting immunizations at day 21
349 and day 42. Serum samples were collected on day 56 for characterization, with flow cytometry
350 occurring between days 56 and 63. In this study, female mice aged 6-10 weeks were used. All
351 experiments were conducted with institutional IACUC approval (MGH protocol 2014N000252).
352
353 Flow Cytometry
354 Spleens were isolated from mice and single cell suspensions were generated by straining through
355 a 70 μm cell strainer. Red blood cells were removed by treating with ACK lysis buffer and washed
356 with PBS. Single cell suspensions were first stained with Aqua Live/Dead amine-reactive dye
357 (0.025 mg/mL) before applying the following B and T cell staining panel using the staining
358 approach described previously (25, 64). This included the following mouse-specific antibodies:
359 CD3-BV786 (BioLegend), CD19-BV421 (BioLegend), IgM-BV605 (BioLegend), IgG-
360 PerCP/Cy5.5 (BioLegend).
361
362 Streptavidin-conjugated fluorophores were used to label the SBP-tagged proteins as probes for
363 flow cytometry. For the cohorts that received the SARS-CoV-2 spike prime followed by either the
364 SARS-CoV-2 RBD homotrimer boost or the RBD homotrimer cocktail boost, the following probes
365 were generated: SARS-CoV-2 RBD-APC/Cy7 (streptavidin-APC/Cy7 from BioLegend), SARS-
366 CoV-2 spike-StreptTactin PE (StrepTactin PE from IBA Lifesciences), SARS-CoV-2 ΔRBM
367 RBD-PE/Cy5.5 (streptavidin-PE/Cy5.5 from BioLegend). The panel for the cohort that received
368 the SARS-CoV-2 spike prime followed by the RBD homotrimer cocktail boost also included

369 SARS-CoV RBD-APC (streptavidin-APC from BioLegend) and WIV1-CoV RBD-BV650
370 (streptavidin-BV650 from BioLegend). For the cohort that received three SARS-CoV-2 spike
371 immunizations, the following probes were generated: SARS-CoV-2 RBD-APC/Cy7 (streptavidin-
372 APC/Cy7 from BioLegend), SARS-CoV-2 spike-StreptTactin PE (StrepTactin PE from IBA
373 Lifesciences), SARS-CoV-2 ΔRBM RBD-APC (streptavidin-APC from BioLegend).
374 Conjugations were performed as previously described (65). Briefly, fluorescent streptavidin
375 conjugates were added in 5 increments with 20 minutes of incubation with rotation at 4°C in
376 between to achieve a final molar ratio of probe to streptavidin valency of 1:1. The final conjugated
377 probe concentration was 0.1 μg/mL. Flow cytometry was performed on a BD FACSAria Fusion
378 cytometer (BD Biosciences). Analysis of the resultant FCS files was conducted using FlowJo
379 (version 10).
380
381 Serum ELISAs
382 Serum ELISAs were performed by coating Corning 96-well clear flat bottom high bind microplates
383 with 100 μL of protein at 5 μg/mL in PBS. Plates were incubated overnight at 4°C. Coating
384 solution was removed, and plates were blocked using 1% BSA in PBS with 1% Tween for 60
385 minutes at room temperature. Blocking solution was removed. Sera were diluted 1:40 in PBS, and
386 5-fold serial dilution was performed. CR3022 IgG at a starting dilution of 5 μg/mL with 5-fold
387 serial dilution was used as a positive control. 40 μL of primary antibody solution was applied to
388 each well. Primary incubation occurred for 90 minutes at room temperature. Plates were then
389 washed three times with PBS-Tween. HRP-conjugated rabbit anti-mouse IgG antibody (Abcam)
390 at a concentration of 1:20,000 in PBS and a volume of 150 μL was used as a secondary antibody.
391 Secondary incubation occurred for 60 minutes at room temperature. Plates were then washed three

392 times with PBS-Tween. 1xABTS development solution (ThermoFisher) was applied as outlined
393 in the manufacturer's recommendations. Development was stopped after 30 minutes with a 1%
394 SDS solution. Plates were read at 405 nm using a SectraMax iD3 plate reader (Molecular Devices).
395
396 Competition ELISAs
397 Competition ELISAs were performed using a similar protocol to serum ELISAs. The primary
398 incubation consisted of 40 μL of the relevant IgG at 1 μM. Incubation occurred at room
399 temperature for 60 minutes. Mouse sera were then spiked in at a final concentration in the linear
400 range of the serum ELISA titration curve (1:800 for the cohort that received three SARS-CoV-2
401 RBD monomer immunizations, 1:12,800 for all other cohorts). Plates were incubated at room
402 temperature for an additional 60 minutes. The primary solution was removed, and plates were
403 washed three times using PBS-Tween. HRP-conjugated goat anti-mouse IgG, human/bovine/horse
404 SP ads antibody (Southern Biotech) was applied at a concentration of 1:4000 and a volume of 150
405 μL as a secondary antibody. Plates were then incubated, washed, and developed using the same
406 procedure as the serum ELISAs.
407
408 ACE2 Cell Binding Assay
409 ACE2 expressing 293T cells (66) (a kind gift from Nir Hacohen and Michael Farzan) were
410 harvested and washed with PBSF. Cells were allocated such that 200,000 cells were labelled for
411 each condition. Cells were incubated with 100 μL of 200 nM antigen in PBS for 60 minutes on
412 ice. Following two washes with PBS supplemented with 2% FBS, cells were incubated with 50
413 μL of 1:200 streptavidin-PE (Invitrogen) on ice for 30 minutes. Cells were washed twice and

414 resuspended in 100 μL of PBS supplemented with 2% FBS. Flow cytometry was performed using
415 a Stratedigm S1000Exi Flow Cytometer. FCS files were analyzed using FlowJo (version 10).
416
417 Human Serum Samples
418 A total of 24 human serum samples were obtained from a previously characterized cohort (9).
419 All patients had received either 1 or 2 doses of the Pfizer (BNT162b2) or Moderna (mRNA-
420 1273) vaccines. Of the patients who had received both doses, samples were collected a median of
421 14 days following the second dose (range: 4 days – 32 days). The median patient age was 51
422 years, with ages ranging from 22-66 years.
423
424 Serum Adsorption
425 SNAP-tagged (61) MERS-CoV RBD, SARS-CoV-2 ΔRBM RBD with four additional putative
426 glycosylation sites (Figure S5), and SARS-CoV-2 RBD were conjugated to SNAP-Capture Pull-
427 Down resin (New England BioLabs). For each conjugation, 20 μL of settled resin was resuspended
428 in 100 μL of protein at 1 mg/mL per the manufacturer's recommendations. Both MERS-CoV RBD
429 and SARS-CoV-2 RBD conjugation reactions also included 1 mM DTT to improve conjugation
430 efficiency. Wildtype-like reactivity to conformationally specific Fabs (CR3022, S309, and B38 for
431 SARS-CoV-2 RBD; m336 for MERS RBD) in the presence of 1 mM DTT was confirmed prior to
432 conjugation (15, 17, 18, 67). Conjugation occurred with rotation overnight at 4°C.
433
434 Following conjugation, the resin was washed 5 times with PBS via resuspension followed by
435 centrifugation and the removal of the supernatant. Sera from the mice in each cohort were pooled
436 and diluted 1:40 in PBS to a total volume of 100 μL. Sera from human patients were diluted 1:20

437 in PBS to a total volume of 100 μL. Diluted sera were added to the conjugated resin and incubated
438 with rotation overnight at 4°C. Resin was filtered from the sera following incubation, and the
439 adsorbed sera was used for neutralization assays and ELISAs.
440
441 Serum Adsorption ELISAs
442 Serum adsorption ELISAs were performed using a similar protocol to the serum ELISAs. For the
443 primary antibody incubation, adsorbed serum solution was diluted 1:2, and subsequent serial 5-
444 fold dilutions were generated. The remainder of the assay was performed according to the serum
445 ELISA procedure.
446
447 Pseudovirus Neutralization Assay
448 Serum neutralization against SARS-CoV-2, SARS-CoV, and WIV1-CoV was assessed using
449 lentiviral particles pseudotyped with the respective spike proteins as previously described (8, 9).
450 Lentiviral particles were produced via transient transfection of 293T cells. The titers of viral
451 supernatants were determined via flow cytometry on 293T-ACE2 cells (66) and via the HIV-1
452 $p24^{CA}$ antigen capture assay (Leidos Biomedical Research, Inc.). Assays were performed in 384-
453 well plates (Grenier) using a Fluent Automated Workstation (Tecan). For mouse sera, samples
454 were initially diluted 1:9, with subsequent serial 3-fold dilutions. For human and mouse sera that
455 had previously been adsorbed, the adsorbed sample was used at an initial 1:3 dilution, and serial
456 3-fold dilutions were performed. Serum sample volume in each well was 20 μL, and 20 μL of
457 pseudovirus containing 125 infectious units was added. The combination was incubated for 60
458 minutes at room temperature. Afterwards, 10,000 293T-ACE2 cells (66) in 20 μL of media

459 containing 15 μg/mL polybrene was added. The plates were then incubated at 37°C for 60-72
460 hours.
461
462 A previously described assay buffer was used to lyse the cells (68). A Spectramax L luminometer
463 (Molecular Devices) was used to quantify luciferase expression. Percent neutralization at each
464 serum concentration was determined by subtracting background luminescence from cells only
465 sample wells, then dividing by luminescence of wells with only virus and cells. GraphPad Prism
466 was used to fit nonlinear regressions to the data, which allowed IC_{50} values to be calculated using
467 the interpolated 50% inhibitory concentration. IC_{50} values were calculated for all samples with a
468 neutralization value of at least 80% at the highest serum concentration.
469
470 Phylogenetic Trees
471 Prior to generating phylogenetic trees, alignments were generated via ClustalOmega. Phylogenetic
472 trees were then generated using those alignments as inputs into a neighbor-joining algorithm via
473 ClustalW2. All settings were left as default.
474
475 Statistical Analysis
476 Statistical analyses and curve fitting were performed using GraphPad Prism (version 9). To
477 compare two populations of continuous variables without evidence of conforming to a normal
478 distribution, the non-parametric two-tailed Mann-Whitney U test was used. To compare multiple
479 populations meeting this description, the Kruskal-Wallis test was used with post hoc analysis using
480 Dunn's multiple comparison testing. The ratio paired t-test was used to compare two populations

481 with evidence of normality. P values were corrected for multiple comparisons, and a p value <

482 0.05 was considered significant.

483

484

485 **References:**

486 1. Amanat F, Krammer F. SARS-CoV-2 Vaccines: Status Report. Immunity.
487 2020;52(4):583-9.
488 2. Anthony SJ, Johnson CK, Greig DJ, Kramer S, Che X, Wells H, et al. Global patterns in
489 coronavirus diversity. Virus Evol. 2017;3(1):vex012.
490 3. Boni MF, Lemey P, Jiang X, Lam TT, Perry BW, Castoe TA, et al. Evolutionary origins
491 of the SARS-CoV-2 sarbecovirus lineage responsible for the COVID-19 pandemic. Nat
492 Microbiol. 2020.
493 4. Origin NRCUCoASGCfSaRtEDoZ. Sustaining Global Surveillance and Response to
494 Emerging Zoonotic Diseases. Keusch GT PM, Gonzalez MC, et al., editor. Washington (DC):
495 National Academies Press (US); 2009.
496 5. Jiang S, Hillyer C, Du L. Neutralizing Antibodies against SARS-CoV-2 and Other
497 Human Coronaviruses. Trends Immunol. 2020;41(5):355-9.
498 6. Du L, He Y, Zhou Y, Liu S, Zheng BJ, Jiang S. The spike protein of SARS-CoV--a target
499 for vaccine and therapeutic development. Nat Rev Microbiol. 2009;7(3):226-36.
500 7. Yang W, Kandula S, Huynh M, Greene SK, Van Wye G, Li W, et al. Estimating the
501 infection-fatality risk of SARS-CoV-2 in New York City during the spring 2020 pandemic wave:
502 a model-based analysis. Lancet Infect Dis. 2020.
503 8. Garcia-Beltran WF, Lam EC, Astudillo MG, Yang D, Miller TE, Feldman J, et al.
504 COVID-19-neutralizing antibodies predict disease severity and survival. Cell. 2021;184(2):476-
505 88 e11.
506 9. Garcia-Beltran WF, Lam EC, St Denis K, Nitido AD, Garcia ZH, Hauser BM, et al.
507 Multiple SARS-CoV-2 variants escape neutralization by vaccine-induced humoral immunity.
508 Cell. 2021.
509 10. Knipe DM, Howley PM. Fields virology. 6th ed. Philadelphia, PA: Wolters
510 Kluwer/Lippincott Williams & Wilkins Health; 2013. 2 volumes p.
511 11. Wec AZ, Wrapp D, Herbert AS, Maurer DP, Haslwanter D, Sakharkar M, et al. Broad
512 neutralization of SARS-related viruses by human monoclonal antibodies. Science. 2020.
513 12. Yuan M, Liu H, Wu NC, Lee CD, Zhu X, Zhao F, et al. Structural basis of a shared
514 antibody response to SARS-CoV-2. Science. 2020.
515 13. Zost SJ, Gilchuk P, Case JB, Binshtein E, Chen RE, Nkolola JP, et al. Potently
516 neutralizing and protective human antibodies against SARS-CoV-2. Nature. 2020.
517 14. Rogers TF, Zhao F, Huang D, Beutler N, Burns A, He WT, et al. Isolation of potent
518 SARS-CoV-2 neutralizing antibodies and protection from disease in a small animal model.
519 Science. 2020.
520 15. Wu Y, Wang F, Shen C, Peng W, Li D, Zhao C, et al. A noncompeting pair of human
521 neutralizing antibodies block COVID-19 virus binding to its receptor ACE2. Science.
522 2020;368(6496):1274-8.
523 16. Du L, Yang Y, Zhou Y, Lu L, Li F, Jiang S. MERS-CoV spike protein: a key target for
524 antivirals. Expert Opin Ther Targets. 2017;21(2):131-43.
525 17. Yuan M, Wu NC, Zhu X, Lee CD, So RTY, Lv H, et al. A highly conserved cryptic
526 epitope in the receptor binding domains of SARS-CoV-2 and SARS-CoV. Science.
527 2020;368(6491):630-3.

528 18. Pinto D, Park YJ, Beltramello M, Walls AC, Tortorici MA, Bianchi S, et al. Cross-
529 neutralization of SARS-CoV-2 by a human monoclonal SARS-CoV antibody. Nature.
530 2020;583(7815):290-5.
531 19. Dai L, Zheng T, Xu K, Han Y, Xu L, Huang E, et al. A Universal Design of
532 Betacoronavirus Vaccines against COVID-19, MERS, and SARS. Cell. 2020;182(3):722-33 e11.
533 20. Menachery VD, Yount BL, Jr., Sims AC, Debbink K, Agnihothram SS, Gralinski LE, et
534 al. SARS-like WIV1-CoV poised for human emergence. Proc Natl Acad Sci U S A.
535 2016;113(11):3048-53.
536 21. Fonville JM, Wilks SH, James SL, Fox A, Ventresca M, Aban M, et al. Antibody
537 landscapes after influenza virus infection or vaccination. Science. 2014;346(6212):996-1000.
538 22. Sliepen K, van Montfort T, Melchers M, Isik G, Sanders RW. Immunosilencing a highly
539 immunogenic protein trimerization domain. J Biol Chem. 2015;290(12):7436-42.
540 23. Pallesen J, Wang N, Corbett KS, Wrapp D, Kirchdoerfer RN, Turner HL, et al.
541 Immunogenicity and structures of a rationally designed prefusion MERS-CoV spike antigen.
542 Proc Natl Acad Sci U S A. 2017;114(35):E7348-E57.
543 24. Corbett KS, Edwards DK, Leist SR, Abiona OM, Boyoglu-Barnum S, Gillespie RA, et al.
544 SARS-CoV-2 mRNA vaccine design enabled by prototype pathogen preparedness. Nature.
545 2020;586(7830):567-71.
546 25. Sangesland M, Ronsard L, Kazer SW, Bals J, Boyoglu-Barnum S, Yousif AS, et al.
547 Germline-Encoded Affinity for Cognate Antigen Enables Vaccine Amplification of a Human
548 Broadly Neutralizing Response against Influenza Virus. Immunity. 2019;51(4):735-49 e8.
549 26. Lan J, Ge J, Yu J, Shan S, Zhou H, Fan S, et al. Structure of the SARS-CoV-2 spike
550 receptor-binding domain bound to the ACE2 receptor. Nature. 2020;581(7807):215-20.
551 27. Barnes CO, Jette CA, Abernathy ME, Dam KA, Esswein SR, Gristick HB, et al. SARS-
552 CoV-2 neutralizing antibody structures inform therapeutic strategies. Nature. 2020.
553 28. Menachery VD, Yount BL, Jr., Debbink K, Agnihothram S, Gralinski LE, Plante JA, et
554 al. A SARS-like cluster of circulating bat coronaviruses shows potential for human emergence.
555 Nat Med. 2015;21(12):1508-13.
556 29. Shang J, Ye G, Shi K, Wan Y, Luo C, Aihara H, et al. Structural basis of receptor
557 recognition by SARS-CoV-2. Nature. 2020;581(7807):221-4.
558 30. Cohen AA, Gnanapragasam PNP, Lee YE, Hoffman PR, Ou S, Kakutani LM, et al.
559 Mosaic nanoparticles elicit cross-reactive immune responses to zoonotic coronaviruses in mice.
560 Science. 2021;371(6530):735-41.
561 31. Abu-Raddad LJ, Chemaitelly H, Butt AA, National Study Group for C-V. Effectiveness
562 of the BNT162b2 Covid-19 Vaccine against the B.1.1.7 and B.1.351 Variants. N Engl J Med.
563 2021.
564 32. Edara VV, Lai L, Sahoo MK, Floyd K, Sibai M, Solis D, et al. Infection and vaccine-
565 induced neutralizing antibody responses to the SARS-CoV-2 B.1.617.1 variant. bioRxiv. 2021.
566 33. Wu K, Werner AP, Koch M, Choi A, Narayanan E, Stewart-Jones GBE, et al. Serum
567 Neutralizing Activity Elicited by mRNA-1273 Vaccine. N Engl J Med. 2021;384(15):1468-70.
568 34. Collier DA, De Marco A, Ferreira I, Meng B, Datir RP, Walls AC, et al. Sensitivity of
569 SARS-CoV-2 B.1.1.7 to mRNA vaccine-elicited antibodies. Nature. 2021;593(7857):136-41.
570 35. Shapiro J, Dean NE, Madewell ZJ, Yang Y, Halloran ME, Longini I. Efficacy Estimates
571 for Various COVID-19 Vaccines: What we Know from the Literature and Reports. medRxiv.
572 2021.

573 36. Martinez DR, Schaefer A, Leist SR, De la Cruz G, West A, Atochina-Vasserman EN, et
574 al. Chimeric spike mRNA vaccines protect against sarbecovirus challenge in mice. Science.
575 2021.
576 37. Walls AC, Fiala B, Schafer A, Wrenn S, Pham MN, Murphy M, et al. Elicitation of
577 Potent Neutralizing Antibody Responses by Designed Protein Nanoparticle Vaccines for SARS-
578 CoV-2. Cell. 2020;183(5):1367-82 e17.
579 38. Wang W, Huang B, Zhu Y, Tan W, Zhu M. Ferritin nanoparticle-based SARS-CoV-2
580 RBD vaccine induces a persistent antibody response and long-term memory in mice. Cell Mol
581 Immunol. 2021;18(3):749-51.
582 39. Kang YF, Sun C, Zhuang Z, Yuan RY, Zheng Q, Li JP, et al. Rapid Development of
583 SARS-CoV-2 Spike Protein Receptor-Binding Domain Self-Assembled Nanoparticle Vaccine
584 Candidates. ACS Nano. 2021;15(2):2738-52.
585 40. Li H, Guo L, Zheng H, Li J, Zhao X, Li J, et al. Self-Assembling Nanoparticle Vaccines
586 Displaying the Receptor Binding Domain of SARS-CoV-2 Elicit Robust Protective Immune
587 Responses in Rhesus Monkeys. Bioconjug Chem. 2021;32(5):1034-46.
588 41. Liu Z, Xu W, Xia S, Gu C, Wang X, Wang Q, et al. RBD-Fc-based COVID-19 vaccine
589 candidate induces highly potent SARS-CoV-2 neutralizing antibody response. Signal Transduct
590 Target Ther. 2020;5(1):282.
591 42. Yang J, Wang W, Chen Z, Lu S, Yang F, Bi Z, et al. A vaccine targeting the RBD of the
592 S protein of SARS-CoV-2 induces protective immunity. Nature. 2020;586(7830):572-7.
593 43. Ma X, Zou F, Yu F, Li R, Yuan Y, Zhang Y, et al. Nanoparticle Vaccines Based on the
594 Receptor Binding Domain (RBD) and Heptad Repeat (HR) of SARS-CoV-2 Elicit Robust
595 Protective Immune Responses. Immunity. 2020;53(6):1315-30 e9.
596 44. Huang WC, Zhou S, He X, Chiem K, Mabrouk MT, Nissly RH, et al. SARS-CoV-2 RBD
597 Neutralizing Antibody Induction is Enhanced by Particulate Vaccination. Adv Mater.
598 2020;32(50):e2005637.
599 45. Chen RE, Zhang X, Case JB, Winkler ES, Liu Y, VanBlargan LA, et al. Resistance of
600 SARS-CoV-2 variants to neutralization by monoclonal and serum-derived polyclonal antibodies.
601 Nat Med. 2021;27(4):717-26.
602 46. Suryadevara N, Shrihari S, Gilchuk P, VanBlargan LA, Binshtein E, Zost SJ, et al.
603 Neutralizing and protective human monoclonal antibodies recognizing the N-terminal domain of
604 the SARS-CoV-2 spike protein. Cell. 2021;184(9):2316-31 e15.
605 47. Chi X, Yan R, Zhang J, Zhang G, Zhang Y, Hao M, et al. A neutralizing human antibody
606 binds to the N-terminal domain of the Spike protein of SARS-CoV-2. Science.
607 2020;369(6504):650-5.
608 48. Hansen J, Baum A, Pascal KE, Russo V, Giordano S, Wloga E, et al. Studies in
609 humanized mice and convalescent humans yield a SARS-CoV-2 antibody cocktail. Science.
610 2020;369(6506):1010-4.
611 49. Rappazzo CG, Tse LV, Kaku CI, Wrapp D, Sakharkar M, Huang D, et al. Broad and
612 potent activity against SARS-like viruses by an engineered human monoclonal antibody.
613 Science. 2021;371(6531):823-9.
614 50. Greaney AJ, Loes AN, Gentles LE, Crawford KHD, Starr TN, Malone KD, et al.
615 Antibodies elicited by mRNA-1273 vaccination bind more broadly to the receptor binding
616 domain than do those from SARS-CoV-2 infection. Sci Transl Med. 2021.

617 51. Jones BE, Brown-Augsburger PL, Corbett KS, Westendorf K, Davies J, Cujec TP, et al.
618 The neutralizing antibody, LY-CoV555, protects against SARS-CoV-2 infection in nonhuman
619 primates. Sci Transl Med. 2021;13(593).
620 52. Wu LP, Wang NC, Chang YH, Tian XY, Na DY, Zhang LY, et al. Duration of antibody
621 responses after severe acute respiratory syndrome. Emerg Infect Dis. 2007;13(10):1562-4.
622 53. Drosten C, Meyer B, Muller MA, Corman VM, Al-Masri M, Hossain R, et al.
623 Transmission of MERS-coronavirus in household contacts. N Engl J Med. 2014;371(9):828-35.
624 54. Sariol A, Perlman S. Lessons for COVID-19 Immunity from Other Coronavirus
625 Infections. Immunity. 2020;53(2):248-63.
626 55. Schmidt OW, Allan ID, Cooney MK, Foy HM, Fox JP. Rises in titers of antibody to
627 human coronaviruses OC43 and 229E in Seattle families during 1975-1979. Am J Epidemiol.
628 1986;123(5):862-8.
629 56. Monto AS, Lim SK. The Tecumseh study of respiratory illness. VI. Frequency of and
630 relationship between outbreaks of coronavirus infection. J Infect Dis. 1974;129(3):271-6.
631 57. Hendley JO, Fishburne HB, Gwaltney JM, Jr. Coronavirus infections in working adults.
632 Eight-year study with 229 E and OC 43. Am Rev Respir Dis. 1972;105(5):805-11.
633 58. Callow KA, Parry HF, Sergeant M, Tyrrell DA. The time course of the immune response
634 to experimental coronavirus infection of man. Epidemiol Infect. 1990;105(2):435-46.
635 59. Gorman MJ, Patel N, Guebre-Xabier M, Zhu A, Atyeo C, Pullen KM, et al. Collaboration
636 between the Fab and Fc contribute to maximal protection against SARS-CoV-2 in nonhuman
637 primates following NVX-CoV2373 subunit vaccine with Matrix-M vaccination. bioRxiv. 2021.
638 60. Weisblum Y, Schmidt F, Zhang F, DaSilva J, Poston D, Lorenzi JC, et al. Escape from
639 neutralizing antibodies by SARS-CoV-2 spike protein variants. Elife. 2020;9.
640 61. Keppler A, Gendreizig S, Gronemeyer T, Pick H, Vogel H, Johnsson K. A general
641 method for the covalent labeling of fusion proteins with small molecules in vivo. Nat Biotechnol.
642 2003;21(1):86-9.
643 62. Schmidt AG, Do KT, McCarthy KR, Kepler TB, Liao HX, Moody MA, et al.
644 Immunogenic Stimulus for Germline Precursors of Antibodies that Engage the Influenza
645 Hemagglutinin Receptor-Binding Site. Cell Rep. 2015;13(12):2842-50.
646 63. Schmidt AG, Therkelsen MD, Stewart S, Kepler TB, Liao HX, Moody MA, et al. Viral
647 receptor-binding site antibodies with diverse germline origins. Cell. 2015;161(5):1026-34.
648 64. Weaver GC, Villar RF, Kanekiyo M, Nabel GJ, Mascola JR, Lingwood D. In vitro
649 reconstitution of B cell receptor-antigen interactions to evaluate potential vaccine candidates. Nat
650 Protoc. 2016;11(2):193-213.
651 65. Kaneko N, Kuo HH, Boucau J, Farmer JR, Allard-Chamard H, Mahajan VS, et al. Loss
652 of Bcl-6-Expressing T Follicular Helper Cells and Germinal Centers in COVID-19. Cell.
653 2020;183(1):143-57 e13.
654 66. Moore MJ, Dorfman T, Li W, Wong SK, Li Y, Kuhn JH, et al. Retroviruses pseudotyped
655 with the severe acute respiratory syndrome coronavirus spike protein efficiently infect cells
656 expressing angiotensin-converting enzyme 2. J Virol. 2004;78(19):10628-35.
657 67. Ying T, Du L, Ju TW, Prabakaran P, Lau CC, Lu L, et al. Exceptionally potent
658 neutralization of Middle East respiratory syndrome coronavirus by human monoclonal
659 antibodies. J Virol. 2014;88(14):7796-805.
660 68. Siebring-van Olst E, Vermeulen C, de Menezes RX, Howell M, Smit EF, van Beusechem
661 VW. Affordable luciferase reporter assay for cell-based high-throughput screening. J Biomol
662 Screen. 2013;18(4):453-61.

Acknowledgments: We thank members of the Schmidt and Lingwood Laboratories for helpful discussions. We thank Dr. Jason McLellan from University of Texas, Austin for the spike plasmid. We thank Nir Hacohen and Michael Farzan for the kind gift of the ACE2 expressing 293T cells to ABB.; **Funding:** We acknowledge funding from NIH R01s AI146779 (AGS), AI124378, AI137057 and AI153098 (DL), and a Massachusetts Consortium on Pathogenesis Readiness (MassCPR) grant (AGS); training grants: NIGMS T32 GM007753 (BMH and TMC); T32 AI007245 (JF); F31 Al138368 (MS). A.B.B. is supported by the National Institutes for Drug Abuse (NIDA) Avenir New Innovator Award DP2DA040254, the MGH Transformative Scholars Program as well as funding from the Charles H. Hood Foundation. This independent research was supported by the Gilead Sciences Research Scholars Program in HIV.; **Author contributions:** Conceptualization, BMH, MS, JF, TMC, DL, AGS; Methodology, BMH, ECL, TMC, ABB, DL, AGS; Investigation, BMH, MS, ECL, KSD, JF, ASY, TK; Writing – Original Draft, BMH and AGS; Writing – Review and Editing, all authors; Funding Acquisition, ABB, DL, AGS; Supervision, ABB, DL, AGS.; **Competing interests:** Authors declare no competing interests.; and **Data and materials availability:** All data is available in the main text or in the supplementary materials.

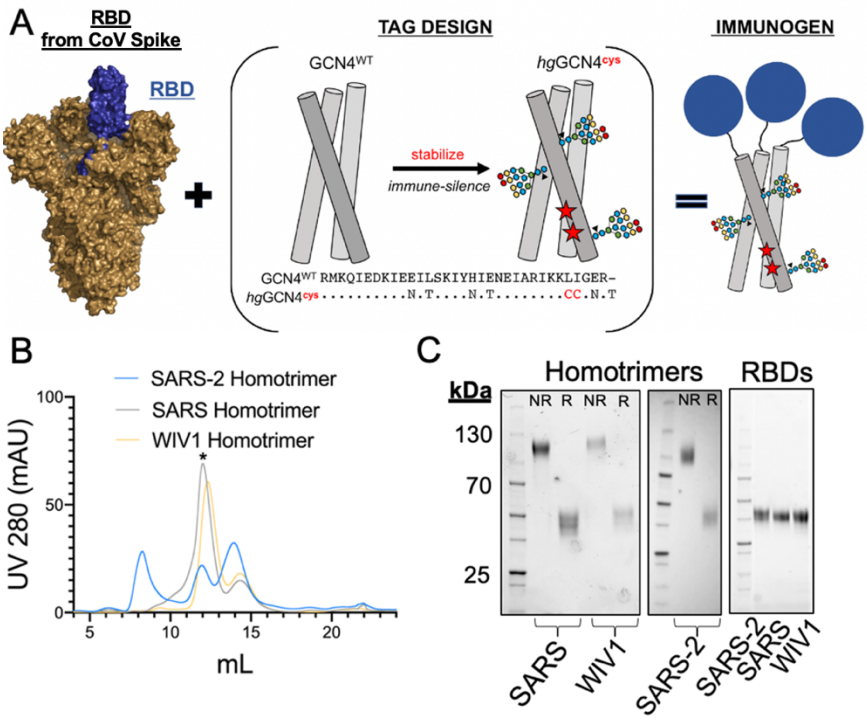

Fig. 1. Immunogen design, expression, and purification. (**A**) Design schematic for generating RBD homotrimers appended onto a cystine-stabilized (red stars) hyperglycosylated GCN4 tag. (PDB: 6VSB) (**B**) Representative size exclusion trace with (*) marking the homotrimeric construct. Fractions in this peak were pooled and used for immunizations. **(C)** SDS-PAGE analysis of purified homotrimers following removal of the affinity purification tags under non-reducing (NR) and reducing (R) conditions. The engineered disulfide bond at the C-terminus of the hyperglycosylated GCN4 tag separated under reducing conditions. Panel includes monomeric RBDs run under reducing conditions for comparison. (Related to **Fig. S1**)

A

Cohort ID	Day 0	Day 21	Day 42
Spike	SARS-2 Spike	SARS-2 Spike	SARS-2 Spike
RBD	SARS-2 RBD	SARS-2 RBD	SARS-2 RBD
Homotrimer	SARS-2 Spike	SARS-2 Homotrimer	SARS-2 Homotrimer
Cocktail	SARS-2 Spike	RBD Homotrimer Cocktail	RBD Homotrimer Cocktail

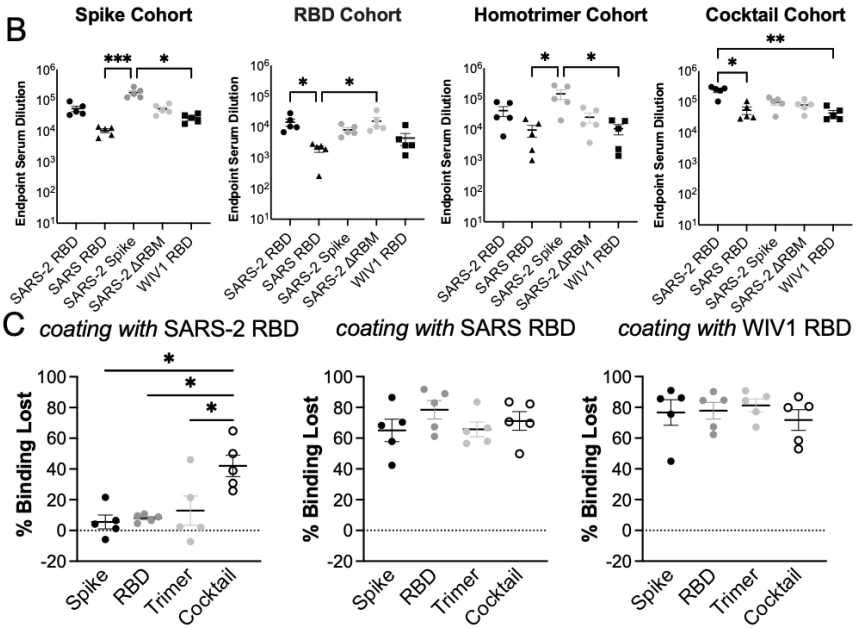

692

693 **Fig. 2. Serum response to immunization regimens.** (**A**) Four immunization cohorts were used
694 for this study (n=5 mice, per cohort). (**B**) Serum was assayed in ELISA at day 56 with different
695 coronavirus antigens. (**C**) Percent of binding lost in competition ELISAs using S309 and CR3022
696 vs. no IgG and SARS-CoV-2, SARS-CoV, and WIV1-CoV RBDs as coating antigens. Statistical
697 significance was determined using Kruskal-Wallis test with post-hoc analysis using Dunn's test
698 corrected for multiple comparisons (* = $p < 0.05$, ** = $p < 0.01$, *** = $p < 0.001$); ns = not
699 significant. (Related to **Fig. S2**)

700

701

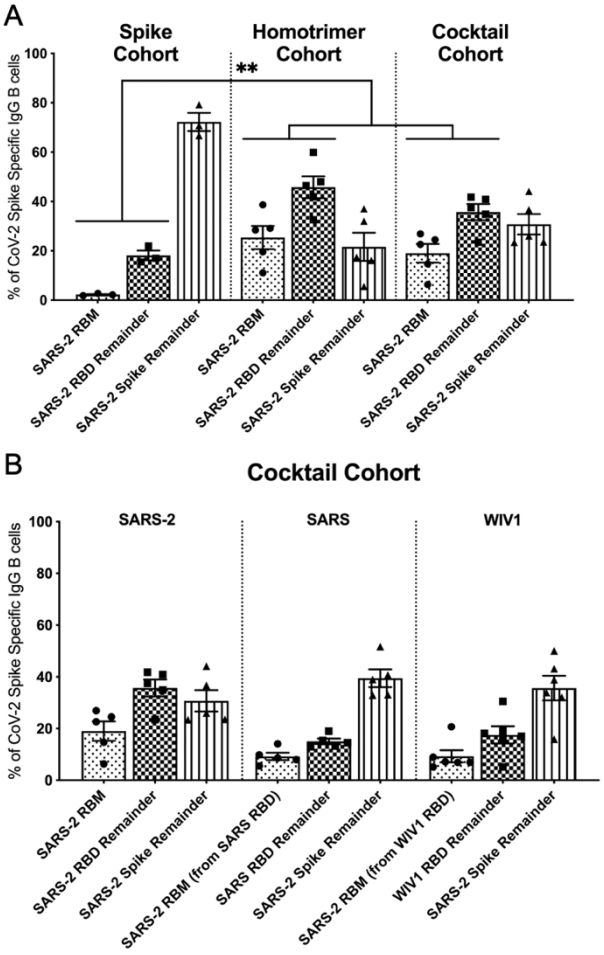

702

703

704 **Fig. 3. SARS-CoV-2-specific IgG B cells expanded following immunization. (A)** Spike-
705 directed responses were binned into RBM, RBD remainder (excluding RBM epitopes), and spike
706 remainder (excluding RBD and RBM epitopes) populations using relevant probes in flow
707 cytometry. Data is shown as a percentage of total spike-specific IgG B-cells. We evaluated the
708 distribution of SARS-CoV-2 spike-directed responses and found evidence of focusing towards
709 non-spike RBD epitopes in the cohorts boosted with the SARS-CoV-2 RBD homotrimer and the
710 RBD homotrimer cocktail versus the cohort that received three SARS-CoV-2 spike immunizations
711 ($p = 0.0070$ via Mann-Whitney U test) (A). (**B**) The cocktail cohort was additionally assayed for
712 SARS-CoV or WIV1-CoV RBD reactivity, as described in (**A**). (Related to **Fig. S3**)

713

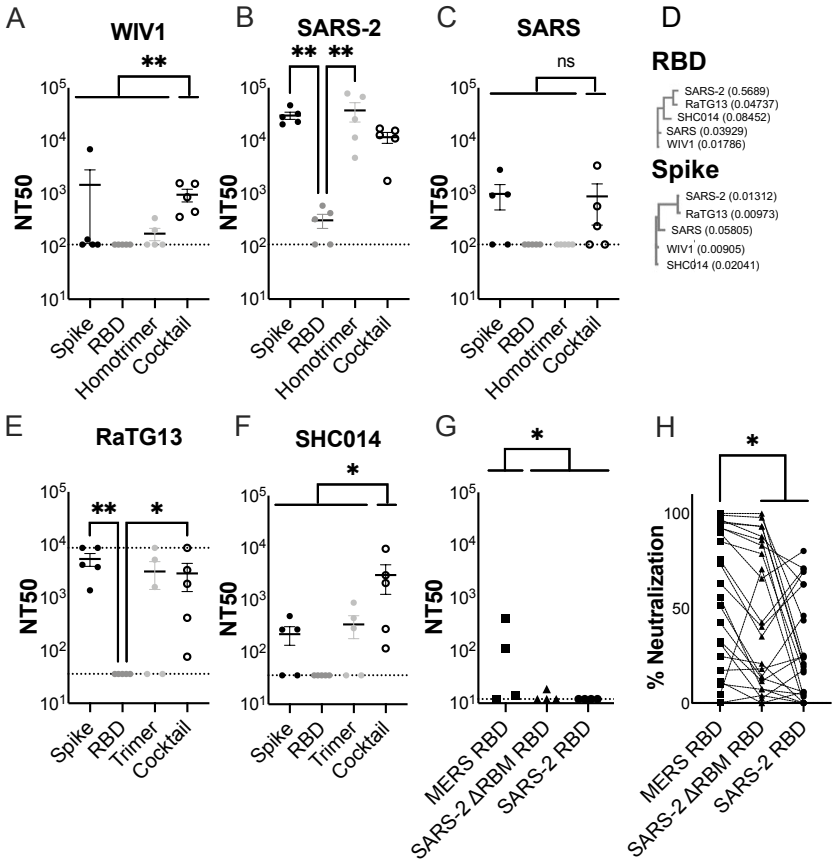

Fig. 4. Pan-sarbecovirus serum neutralization using pseudoviruses. Day 56 serum from each cohort was assayed for neutralization against (**A**) WIV1-CoV, (**B**) SARS-CoV-2, (**C**) SARS-CoV, (**E**) RaTG13-CoV, and (**F**) SHC014-CoV pseudoviruses. For the SARS-CoV-2 (**B**) and RaTG13-CoV (**E**) pseudoviruses, statistical significance was determined using Kruskal-Wallis test with post-hoc analysis using Dunn's test; * = $p < 0.05$, ** = $p < 0.01$. There was a significant difference in WIV1-CoV neutralization (Mann-Whitney U test; $p = 0.0012$) (**A**) and SHC014-CoV neutralization (Mann-Whitney U test; $p = 0.0145$) (**F**), but there was no significant difference in SARS-CoV neutralization between the control cohorts and the RBD homotrimer cocktail boost cohort (Mann-Whitney U test; $p = 0.2370$) (**C**). (**D**) Neighbor-joining phylogenetic trees were generated to describe the phylogenetic relationships between the RBDs and spikes of the coronaviruses used in this neutralization panel. Branch lengths are displayed in parentheses. (**G**) Serum adsorption to remove antibodies from pooled sera from each mouse cohort directed towards MERS-CoV RBD (negative control), SARS-CoV-2 ΔRBM RBD, and SARS-CoV-2 RBD. Sera

730 adsorbed with MERS-CoV RBD had significantly greater neutralization than those adsorbed with
731 SARS-CoV-2 ΔRBM RBD and SARS-CoV-2 RBD (Mann-Whitney U test; $p = 0.0343$). (**H**) Same
732 assay in (**G), except on immune sera from humans who received** the Pfizer (BNT162b2) or
733 Moderna (mRNA-1273) vaccine (Mann-Whitney U test; $p = 0.0253$). In (**H**), percent neutralization
734 was assessed at a 1:3 dilution of the adsorbed sample. Negative percent neutralization values in
735 (**H**) were set to zero to facilitate analysis. (Related to **Fig. S4**)
736
737